ELSEVIER

Thermochimica Acta 302 (1997) 165–180

thermochimica acta

Applications of scanning microcalorimetry in biophysics and biochemistry

Valery L. Shnyrov[a], Jose M. Sanchez-Ruiz[b], Boris N. Boiko[c], Galina. G. Zhadan[a], Eugene A. Permyakov[c,*]

[a] *Departamento de Bioquímica y Biología Molecular, Universidad de Salamanca, 37007 Salamanca, Spain*
[b] *Departamento de Química Física, Facultad de Ciencias e Instituto de Biotecnologia, Universidad de Granada, 18071 Granada, Spain*
[c] *Institute for Biological Instrumentation, Russian Academy of Sciences, 142292 Pushchino, Moscow region, Russia*

Received 14 November 1996; accepted 29 May 1997

Abstract

Scanning calorimetry is a very powerful and convenient technique for studying temperature-induced conformational transitions in biological systems. The present paper reviews recent applications of the microcalorimetry method in biochemistry and biophysics. © 1997 Elsevier Science B.V.

Keywords: Calorimeter; DSC; Phase transition; Thermal stability; Thermodynamics

1. Introduction

Scanning microcalorimetry occupies a central role in studies on the energetics of biopolymer stabilization. The method permits not only an accurate and direct measurement of the overall thermodynamic parameters such as transition enthalpies, entropies and temperatures, but can also provide fundamental information concerning the mechanisms of temperature-induced transitions. Early on in the development of scanning microcalorimetry, the method was mostly applied to simple systems, such as single-domain low molecular mass proteins. Later, the resolution of complex heat capacity profiles into individual components as well as application of statistical thermodynamic analytical methods permitted the study of much more sophisticated biological objects such as multidomain and multisubunit proteins, membranes and membrane-protein complexes, nucleic acids and DNA-protein complexes, and even cells and tissues. The aim of the present review is to show how the microcalorimetry method is applied in modern biochemistry and biophysics, what kind of information it can provide, and what the perspectives of further developments of this method are.

2. Differential scanning microcalorimeters: Design and operation principles

The operation principle of a differential scanning microcalorimeter is as follows. One of two identical cells in the instrument is filled with the sample under investigation and the other is filled with a reference sample. These cells are heated up by identical heat flows. If the two samples are identical in their thermodynamic properties, the temperature inside the cells will change identically; however, if the samples differ

*Corresponding author.

PII S0040-6031(97)00238-4

in such properties, a difference in the temperatures between them will appear. A special electronic system changes the heating regime of the cells in such a way that the temperatures inside them are equalized. The value of the additional (differential) heat flow required for such temperature compensation is measured by the scanning microcalorimeter. The temperature dependence of the differential heat flow (in power units) is called a thermoanalytical curve and this reflects a difference in the properties of the sample under investigation and the reference sample. Such differences can arise from changes in the phase state, structure and heat capacity of the samples. Since in most scanning calorimeters the temperature scanning rate is constant, the time integral of the measured differential heat flow corresponds to the difference of the changes in the internal energies of the substance under investigation and the reference substance in the integration temperature interval.

The design of scanning calorimeters varies considerably owing to differences in the properties of the substances under investigation, the required temperature region, and the magnitudes of the thermal effects. Despite essential differences in the design of microcalorimeters, they are all characterized by a common set of metrological parameters which, conditionally, can be divided into three groups.

The first group consists of the parameters characterizing temperature changes and temperature measurement: working temperature region, temperature scanning rates, the accuracy of maintaining of the scanning rates, and the accuracy of temperature measurement.

The second group consists of parameters characterizing the heat flow scale: the system for measuring differential heat flow, reproducibility of the base line, sensitivity, and noise level.

The third group relates to parameters characterizing the measuring cells and samples used: the phase state, volume and mass, the material from which the cells are constructed, and so on.

These, then, are the main parameters characterizing a microcalorimeter. The set, however, is incomplete, primarily because of the absence of a system of standard samples for the determination of all the constituents involved in the accuracy of measurement.

Let us consider a typical design of scanning microcalorimeters, using as examples the instruments of the

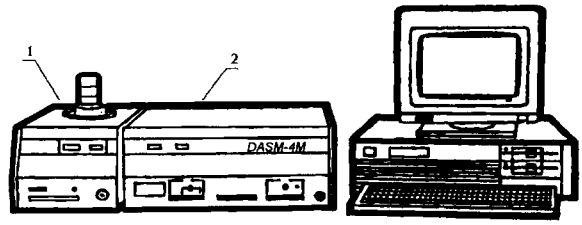

Fig. 1. DASM-4M microcalorimeter.

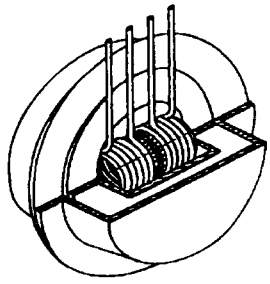

Fig. 2. Calorimetric assembly of the DASM-4M microcalorimeter.

DASM and DSM series, designed and manufactured for many years at the Institute for Biological Instrumentation of the Russian Academy of Sciences.

The DASM-4M microcalorimeter is designed as a bench-type instrument consisting of two units (Fig. 1): (1) *calorimetric unit*, and (2) *measuring unit*.

The main element of the calorimetric unit is a *calorimetric assembly* (Fig. 2). The calorimetric assembly of DASM microcalorimeters consists of a *hermetically sealed vessel* with two *calorimetric cells* placed inside this vessel and identical to one another as regards both, their mass and volume. The cells are surrounded by two concentric *adiabatizing shields* and a *thermostat*. Adiabatization of the cells provides the high sensitivity of the instrument. The cells are made of a platinum capillary (outer diameter 1.6 mm) bent into a cylindrical spiral. The capillary ends are brought out to the filling chamber which is situated in the upper part of the hermetically sealed vessel.

Each calorimetric cell has two *bifilar heaters*, one of which is used for heating the cell and for compensating the difference in the heat power of the two cells. The second heater of one of the cells serves for calibration of the instrument while the second heater

of the second cell serves for compensation of the constant constituent of the difference in the heating rates of the two cells.

A metallic *thermopile* is used to convert the temperature difference between the two cells into an electric signal. A set of thermopiles is used to convert the temperature difference between each adiabatizing shield and the corresponding calorimetric cell. The temperature of the adiabatizing shields is adjusted by means of electric heaters distributed uniformly over the surface of the shields. Thermostat temperature is maintained at a preset value by means of two semiconductor thermopiles. The temperature of the supporting junctions of the thermopiles is stabilized by through-flowing water. A copper resistance thermometer is used as an initial converter of thermostat temperature. A similar thermometer located on the inner adiabatizing shield is used to measure the temperature in the calorimetric cells.

Two centrifugal fans are used to cool down the calorimetric cells and the adiabatizing shields. Intensive circulation of air between the outer adiabatizing shield and the thermostat enables reductions in the time of heating of the instrument up to the initial operating temperature.

The calorimetric cells of the microcalorimeter are heated at a constant rate. One of the cells contains the solution under investigation and the other one is filled with a reference solution. The thermal power difference between the calorimetric cells is compensated electrically using a compensation bridge circuit.

If the thermal properties of the solutions contained in the measuring and reference cells are different, this will cause a *temperature difference between the cells* during the heating process. The temperature difference is converted by the thermocouples of the cells into an *electric signal*, which is amplified by a preamplifier and is then sent to the heating-and-compensation board controlling the heating currents in the cells in order to minimize the temperature difference between the cells. *The voltage proportional to the compensation power* is obtained from the heating and compensation board and is registered by the Y input of a recorder.

Temperature is measured by a resistance thermometer located on the inner adiabatizing shield. The resistance value of this thermometer is converted into voltage by a converter on the converter board. The voltage arrives at the X input of the recorder. A typical calorimetric recording is shown in Fig. 3.

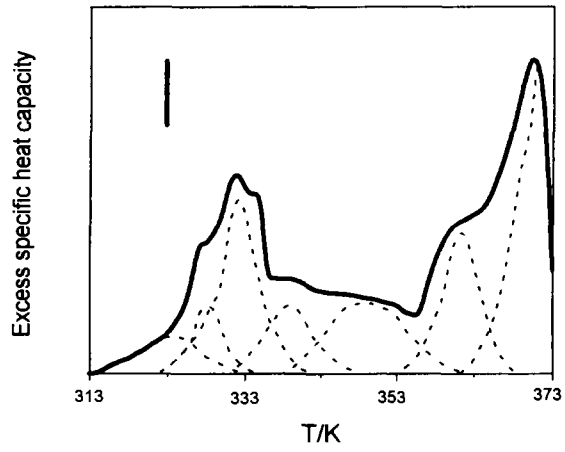

Fig. 3. Heat sorption curve for a suspension of cock sperm and its decomposition into elementary components. DASM-4 microcalorimeter; scan rate 1 K/min; vertical bar corresponds to 10^{-3} J/K; concentration was 2×10^9 cells/ml.

To calibrate the microcalorimeter against the differential power, a known amount of power is supplied to the additional heater of the measuring cell. Each time this happens, a calibration step is measured on the recorder, thus affording the differential power value for the process under investigation.

In order to exclude artifacts due to the release of gas from the solutions during the heating process and to prevent liquids from boiling at high temperatures, extra pressure must be applied to the cells.

There are two cup-like gold cells inside the calorimetric assembly of DSM type calorimeters (Fig. 4). The sample under investigation and a reference sample sealed inside disk-shaped aluminum capsules are placed inside the cells. Thermosensitive transducers

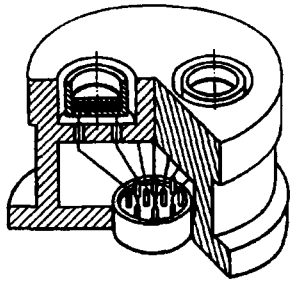

Fig. 4. Calorimetric assembly of the DSM-3A microcalorimeter.

(platinum resistance thermometers) and heating elements are located at the lower part of the assembly. The heaters and the platinum resistance thermometers are connected to the measuring and controlling blocks of the instrument.

During heat production or heat sorption in the sample, the resistance thermometers, which are connected to a highly sensitive electronic bridge circuit of the compensation and scanning regulator, measure small temperature differences between the two cells. After amplification, the signal controls the heating elements of the calorimetric cells to achieve a compensation of the temperature difference. The compensation current is directly proportional to the power of the measured thermal effect.

3. Applications of microcalorimetry to protein and peptide systems

In the initial stage of its use, the differential scanning calorimetry (DSC) method was first applied to study small proteins with reversible thermal transitions. This work provided fundamental information about the thermodynamic properties of protein molecules: the correct enthalpies and entropies of thermal denaturation processes, the contributions of several molecular interactions to the stability of proteins, the correlations between the thermodynamic and structural features of proteins, the main principles of protein energetics, and so on. Many excellent reviews addressing these issues have been published [1–8] and, hence, we shall not go into them any further.

Fundamental studies of the protein energetics still continue. For example, Gomez et al. [9] analyzed the absolute heat capacity of proteins in different conformations. Their results indicate that three major terms account for the absolute heat capacity of a protein:

1. a term that depends only on the primary structure of a protein and contains contributions from vibrational frequencies arising from the stretching and bending modes of each valence bond and internal rotations (up to 85%);
2. a term that contains the contributions of noncovalent interactions arising from secondary and tertiary structures (about 3%); and
3. a term that contains the contributions of hydration (15 to 40%).

The change in heat capacity upon unfolding is primarily given by the increase in the hydration term (ca. 95%) although, to much lesser extent, also by the loss of noncovalent interactions (up to 5%). The major contribution of hydration to the unfolding heat capacity change has also been described by Privalov and Makhatadze [10]. Wintrode et al. [11] studied the energetics of ubiquitin unfolding. For the first time it was shown directly that the enthalpy of protein unfolding is a nonlinear function of temperature. These authors have found that the energy of hydrogen bonding correlates with the average length of the hydrogen bond in a given protein structure. Makhatadze et al. [12] studied the thermodynamics of unfolding of the all β-sheet protein interleukin-1β. Analysis of the reversible unfolding of interleukin-1β shows that the heat denaturation is well approximated by a two-state transition and is accompanied by a significant increase in heat capacity. The partial heat capacity of denatured interleukin-1β is very close to that expected for the completely unfolded protein. It was shown that the Gibbs energy of a hydrogen bond in a β-sheet structure is greater than in α-helices.

Another fundamental issue that has received much attention in recent years is related to the analysis of irreversible DSC transitions. It is generally accepted that the analysis of DSC thermograms according to equilibrium thermodynamics is applicable to those cases in which calorimetric reversibility is found. It should be recognized, however, that the thermal denaturation of proteins is very often irreversible, as shown by the lack of thermal effects in a reheating run of the sample. Irreversibility in protein denaturation is usually attributed to alterations (autolysis, aggregation, chemical alteration of residues, etc., see Ref. [13]) that lock the protein in a state (the final state: F) that is unable to fold back to the native structure. (It should be stressed, however, that in some cases the lack of reproducibility between the first and second scans may be due to the fact that the native state is not at the global Gibbs energy minimum, see Ref. [14].) Irreversible alterations are fundamentally kinetic processes that must be described by rate equations. In the past, it was often assumed that these irreversible alterations were slow and that they did not take place

significantly during the comparatively short time the protein spends in the region; in fact, theoretical simulations of Lumry–Eyring models [4,15–17] suggest that, in some cases, calorimetrically irreversible DSC transitions might be amenable to equilibrium thermodynamic analysis. However, experimental work has indicated that irreversible DSC transitions are very often highly distorted by the kinetics of the irreversible protein alterations, as shown by the strong scanning-rate effects found in many cases [17–30] and by the correlation between the DSC-detected thermal effect and the extent of irreversible denaturation measured by other methods [17,21,22,29,30]. In fact, in many cases [18–21,25–30], the experimental calorimetric data are found to conform to a very simple kinetic model in which only the native (N) and the irreversibly denatured (F) states are significantly populated and the denaturation process can be described entirely by a first-order rate equation: $N \rightarrow F$ and $d[N]/dt = -kt$, where the first-order rate constant (k) depends on temperature and, therefore, on time for DSC experiments, which implies a change in temperature with time according to a given scanning-rate. Theoretical studies [16] show that this 'two-state irreversible model' is in fact a limiting case of more complex Lumry–Eyring-type of models. It is interesting that the kinetic approach has recently been employed by Miles et al. [31] in the analysis of DSC curves corresponding to the irreversible thermal denaturation of collagen fibrils.

As long as denaturation is a reversible equilibrium process, analysis of the DSC data affords a complete energetic characterization of protein stability. Nevertheless, denaturation Gibbs energies (ΔG) are very often determined from non-calorimetric experimental studies on urea- or guanidine-induced denaturation; in particular, in protein engineering studies (see, e.g. Ref. [32]). It should be recognized that solvent-denaturation studies have some advantages:

1. They are fast and simple;
2. Irreversibility is often found in the thermal denaturation of proteins and, in many cases, precludes the equilibrium thermodynamic analysis of DSC curves (see above); in contrast, some of the processes responsible for irreversibility (such as aggregation) are less likely to occur in denaturing concentrations of urea or guanidine; and
3. When based on fluorescence measurements, solvent-denaturation experiments may be carried out with protein concentrations in the micromolar range, which is convenient for work with valuable samples and further disfavors aggregation.

The main drawback of the solvent-denaturation method is that extrathermodynamic assumptions must be employed in the data analysis. Thus, besides the assumption of two-state behaviour, the dependence of the denaturation Gibbs energy on the denaturant concentration is usually assumed to be linear outside the transition region. The validity of this linear extrapolation method (LEM) has been discussed from the theoretical and experimental points of view, but no clear conclusions have yet emerged. Thus, according to several recent studies [33–35], the LEM may significantly under- or overestimate the 'true' ΔG value, as determined in DSC. On the other hand, Myers et al. [36] have reported that in many studies on protein denaturation at low denaturant concentrations no significant deviations from linearity are observed and that there is no justification for using more complex extrapolation methods, unless deviation from the LEM is demonstrated experimentally for a particular protein. The reader is referred to recent works in the field [34–37] for further details on this conflictive issue.

A promising approach to the principles of protein stability with the aim of gaining insight into the nature of underlying molecular interactions is the thermodynamic characterization of the unfolding process of point-mutated proteins. An impressive number of results has been obtained about the thermodynamic effects of changes in the number of disulfide bonds (see, e.g. Refs. [38–40]), about the contribution of hydrogen bonds to conformational stability (see, e.g. Refs. [41,42]), and about the influence of perturbations of the hydrophobicity of the protein (see, e.g. Refs. [43,44]).

Steif et al. [45] studied the structural and energetic perturbations caused by cavity-creating mutations (Leu41 → Val and Leu41 → Ala) in the dimeric 4-α-helical-bundle protein ROP. They evaluated the mutation-induced shifts in the stability parameters and concluded that the mutational effects are predominantly manifested in the native rather than the unfolded state. Ladbury et al. [46] demonstrated that substitution of charged residues in the hydrophobic

core of *Escherichia coli* thioredoxin results in a change in the heat capacity of the native protein. Those authors presented data indicating that this reduction in heat capacity is attributable to structural perturbations, resulting in localized unfolding of the native protein and exposure of residues buried in the wild-type protein to the solvent.

Liggins et al. [47] studied the effects of regional sequence differences on the thermal stability of a globular protein. Thermal transitions have been measured for two isozymes of yeast cytochrome *c* and three composite proteins in which amino-acid segments are exchanged between the parental isozymes. The authors showed that

1. in the temperature range of the unfolding transitions (40-60°C) the unfolding free energies of the composite proteins are only slightly different from those of the parental isozymes,
2. long-range structural effects are responsible for at least some of the observed differences in stability, and
3. changes in ionization of His26 appear to be linked to thermal unfolding.

Hu et al. [48] used three mutants of phage T4 lysozyme to test the prediction that certain residues replacing other residues, at positions where no strain or other unfavorable effects would be caused by the replacement, would decrease the configuration entropy of the unfolded form and thus lead to an apparent stabilization of the native form of the protein. The mutants A82P, A93P, and G113A all show small apparent stabilization at pH 2.5 and 46.2°C (the denaturation temperature of the wild-type protein). The double mutant C54T : C97A shows a weak apparent destabilization. The enthalpy changes produced by these mutations are, in general, much larger than the corresponding free energy changes and, frequently, of opposite sign.

Calorimetric study of the effect of stabilizing osmolytes on protein stability was initiated by Bolen et al. [37,49,50]. Stabilizing osmolites are substances produced at comparatively low concentrations by some living organisms when subjected to denaturing stresses (heat, freezing, high urea concentration, etc.) and these compounds have the interesting property of enhancing protein stability (in a non-specific manner) with no detrimental effects on biological activity. This stabilizing effect is very probably related to the fact that such substances are preferentially excluded from the protein surface (i.e. they cause preferential hydration of the protein, an effect that should favor the protein state with the least surface exposed (see, Ref. [51])). In an important work, Santoro et al. [49] showed that the stabilizing effect of osmolytes may extend well beyond their physiological concentration range; thus, several-molar concentrations of glycine-based osmolytes were found to produce very large increments (up to ca. 20°) in the denaturation temperature of model globular proteins. A detailed characterization of the effect of the osmolyte sarcosine on the denaturation energetics of ribonuclease *a* has recently been reported on the basis of DSC data [52]. The authors of this work found that the denaturation heat capacity increases with the sarcosine concentration and that the effects of temperature and sarcosine concentration on the denaturation enthalpy and entropy are well described by convergence equations (see Refs. [1,7,53]), with a temperature convergence of ca. 100°C for the enthalpy and of ca. 112°C for entropy. This suggests that such effects might be related to a solvent-induced alteration of the apolar-group-hydration contribution [8] to the folding energetics. The study also suggested the possibility of using cosolvent effects on thermal denaturation to evaluate the degree of hydration of denatured proteins.

The microcalorimetry method has been successfully used for studies on multidomain proteins. For example, it has been used to study the structural features of the myosin molecule, which consists of a globular head and a long coiled tail. The myosin subfragment 1 (S1) is an isolated myosin head, i.e. the segment of the myosin molecule containing the sites responsible for ATPase activity and actin binding. Trypsin and other proteinases cleave the S1 heavy chain into three fragments of 25 kDa, 50 kDa and 20 kDa, which are sometimes referred to as 'domains'. To obtain direct evidence for the existence of independently folded cooperative domains in the S1 molecule, Shnyrov et al. [54,55] studied the thermal denaturation of S1 by DSC using the successive annealing procedure introduced by Shnyrov et al. [56]. The procedure allows one to reveal heat sorption peaks corresponding to separate domains in a protein molecule, i.e. the regions which melt independently of one another. The authors found three such domains in

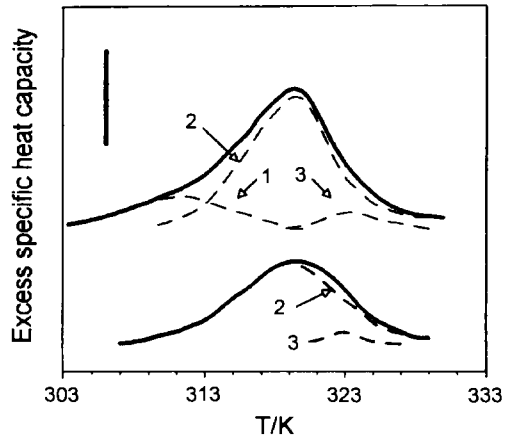

Fig. 5. Heat sorption curves (solid lines) and their decomposition into elementary peaks corresponding to domains 1, 2, and 3 (– dotted lines) for (a) – intact S1 myosin fragment, and (b) – S1 digested by trypsin after methanol treatment (without domain 1). Protein concentration – 2 mg/ml; 10 mM HEPES, pH 7.3; 1 mM $MgCl_2$. DASM-4 microcalorimeter; scan rate – 1 K/min; vertical bar corresponds to 500 J/K kg. Curves are displaced along the ordinate for clarity.

the S1 molecule (Fig. 5). Selective denaturation of the middle 50 kDa segment of the S1 heavy chain by methanol resulted in the disappearance of the heat sorption peak corresponding to the melting of the first, most thermolabile domain. Combining the microcalorimetry method with the intrinsic protein fluorescence technique, they concluded that the most thermolabile domain corresponds to the N-terminal part of the 50 kDa segment of the S1 heavy chain.

Data on the domain structure of the myosin head allowed Levitsky et al. [57] to study the effects of the binding of ADP; a non-hydrolysable analog of ATP, adenosine 5′-[β,γ-imido]triphosphate (AdoPP[NH]P); and orthovanadate (V_i), on the S1 structure. These authors showed that the S1 domain structure in the S1-AdoPP[NH]P and S1-ADP-V_i complexes is similar and differs radically from that of nucleotide-free S1 and S1 in the S1-ADP complex. These data were the first direct evidence that the S1 molecule can adopt two main conformations, which may correspond to different states during ATP hydrolysis.

Nakaya and Watabe [58] used the microcalorimetry method to study the thermal unfolding of myosin and its rod part prepared from carp acclimatized to 10° and 30°C. The transition temperatures of the major peaks for myosin and rod from the 10°C-acclimatized carp were 33.9° and 47.4°C and 33.0° and 44.0°C, respectively. When the data were analyzed in terms of three endotherms, the three transition temperatures obtained for myosin and rod were 32.8°, 34.9°, and 47.4°C and 32.9°, 33.4°, and 44.1°C, respectively. The myosin and rod from carp acclimatized to 30°C showed three distinct peaks at 35.9°, 39.7°, and 49.1°C and 34.5°, 39.7°, and 46.7°C, respectively. The thermal unfolding responsible for these endotherms was mostly explained by melting of the α-helices, as corroborated by CD spectroscopy.

Permyakov et al. [59] studied the thermal denaturation of bovine brain calmodulin using the microcalorimetry method. They found that the heating of apocalmodulin from 5° to 110°C induces at least three unfolding transitions, while the heating of Ca^{2+}-loaded calmodulin causes at least two structural transitions, one of which occurs at relatively low temperatures from ≈30° to ≈50°C. The transitions correspond to calmodulin domains. The data point to the effects of Ca^{2+} binding on the domain structure of calmodulin.

Tanaka et al. [60] used differential scanning calorimetry to study the domain structure of *Aspergillus* glucoamylase. They found that the thermograms for the larger form of the enzyme, G1, and the shorter form which lacks the C-terminal starch-binding domain of G1, G2, could be resolved by assuming two-state unfolding of five and four independent components, respectively. It was shown that there was no domain interaction between the starch-binding and catalytic domains.

Martsev et al. [61] demonstrated that for acid-treated IgG (a large multidomain protein) a pronounced increase (12–15°C) in the thermal stability of the CH2 domain occurs and that this domain no longer shows the separate and thermodynamically independent unfolding at 56°C seen for native IgG. The authors believe that stabilization of the CH2 domain in acid-treated IgG arises from a stronger interaction (relative to the native protein) of the CH2 domain with adjacent and more stable IgG domains.

The domain structure of laccase I from the lignin-degrading basidiomycete PM1 was studied by Coll et al. [62]. They reported three thermal transitions that

could be described by a model of two-state independent unfolding, supporting a three-domain organization of the enzyme. The catalytic site of laccase I is located in the domain with the thermally induced transition at 76°C.

Ruiz-Arribas et al. [63] described three thermodynamically independent domains in xylanase from *Streptomyces halstedii* JM8, each of which follows a two-state thermal unfolding process. Nevertheless, the thermodynamic parameters of unfolding for each domain are inconsistent with some of the correlations obtained for most globular proteins.

An interesting feature of the work of Damaschun et al. [64] is that these authors studied cold denaturation-induced conformational changes in phosphoglycerate kinase from yeast. Decreasing the temperature from 30° to 0°C affects the unfolding of the molecule, a process that involves two stages. Both of them correspond to the successive unfolding of the N-terminal and C-terminal domains. Using a combination of DSC, dynamic light scattering, small-angle X-ray scattering, circular dichroism and fluorescence, these authors have shown that the conformational changes induced by cold denaturation can be described by a transition from a compactly folded molecule to a random coil.

It is sometimes convenient to use isolated structural domains of some proteins for detailed calorimetric studies. For example, Viguera et al. [65] used the SH3 domain of spectrin (ca. 60 residues organized in a β-sheet barrel) to show that its folding and unfolding reactions can be described by a two-state model from both the equilibrium and kinetic points of view. They suggested that the accumulation of kinetic intermediates is merely a result of the size of the protein studied.

The microcalorimetry method is also used to study protein complexes. Musatov et al. [66] used the microcalorimetry method to study the effects of the solubilizing detergent type, pH and temperature on the structure of cytochrome *c* oxidase (10 to 13 non-identical subunits). The data obtained allowed them to conclude that enzyme solubilization by lauryl maltoside gives a more native preparation in comparison with that obtained by solubilization in Tween-80.

Morozova et al. [67,68] studied the thermal denaturation of the muscle calcium-binding protein troponin C in aqueous solution and in the troponin complex, which consists of troponins C, T, and I. Fig. 6a shows

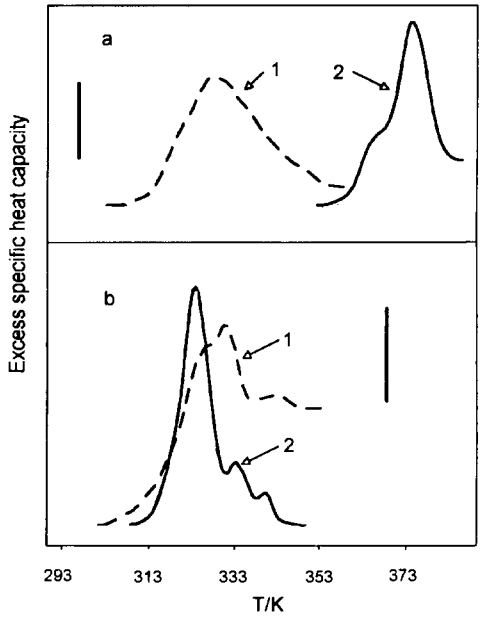

Fig. 6. (a) – Heat sorption curves for troponin I–troponin C complex in the absence of divalent cations (curve 1) and in the presence of 2 mM $CaCl_2$ (curve 2). Protein concentration was 1 mg/ml; 10 mM HEPES, pH 7; vertical bar corresponds to 100 J/K kg. (b) – Heat sorption curves for the troponin complex in the absence of divalent cations (curve 1) and in the presence of 2 mM $CaCl_2$ (curve 2). Protein concentration was 1 mg/ml; 10 mM HEPES, pH 7; vertical bar is 50 J/K kg. DASM-4 microcalorimeter; scan rate 1 K/min.

the heat sorption curves for apo- and Ca^{2+}-loaded troponin C in aqueous solution, while Fig. 6b offers similar data for troponin C within the whole troponin complex. It may clearly be seen that the state of troponin C in solution is completely different from its state in the troponin complex: the binding of Ca^{2+} to free troponin C in solution dramatically increases its thermostability, while the binding of Ca^{2+} to the whole troponin complex causes much smaller changes in thermostability.

DSC has been used to study the thermal stability of the core histone dimer H2A–H2B [69]. The calorimetric data provide a thermodynamic basis to explain previous biochemical and structural observations regarding the stability of the dimer and emphasize the significance of the H2A–H2B interface in the stability of the folded state of the polypeptides of this subunit.

Johnson et al. [70] carried out a thermodynamic analysis of the structural stability of the tetrameric oligomerization domain of p53 tumor suppressor. These authors found that thermal unfolding of the tetramer is reversible and can be described as a two-state transition in which the folded tetramer is converted directly into unfolded monomers. The transition temperature of unfolding was found to be highly dependent on the protein concentration and to follow the expected behavior for a tetramer that dissociates upon unfolding. The authors concluded that the tetramer is essentially stabilized by intersubunit interactions rather than intrasubunit interactions.

The scanning microcalorimetry method can be used to study interactions of proteins with DNA. Davis et al. [71] investigated Pf1 and Fd gene 5 proteins and their single-stranded DNA complexes by NMR spectroscopy and DSC. The thermal stability of both Pf1 and Fd gene proteins is increased by 8°C in the complex with DNA and the nature of the transition is highly cooperative.

As already mentioned, the microcalorimetry method is used to study the interactions of proteins with ions and low molecular-mass organic and inorganic compounds. Permyakov et al. [72] studied the binding of calcium and zinc ions to human and bovine α-lactalbumin. Fig. 7 depicts the heat sorption curves for human α-lactalbumin in different metal-bound states. First, it is clearly seen from the figure that the binding of calcium dramatically increases the thermal stability of α-lactalbumin. An increasing zinc-ion concentration shifts the heat sorption curves to lower temperatures, converting them to multicomponent curves. The heat sorption curves for α-lactalbumin in different states have been decomposed into elementary components using the successive annealing procedure [56]. The heat sorption curves for the Ca^{2+}- and apo-forms as well as for the Ca^{2+}-loaded protein in the presence of high zinc concentrations were single-component, while all other heat sorption curves were multicomponent, corresponding to two or three distinct Zn^{2+}-bound forms of α-lactalbumin. From these experiments, the authors concluded that α-lactalbumin possesses several successively filled Zn^{2+}-binding sites. The destabilizing effect of the zinc and copper ions binding to the protein structure was also found with the microcalorimetry method for aminoacylase [73].

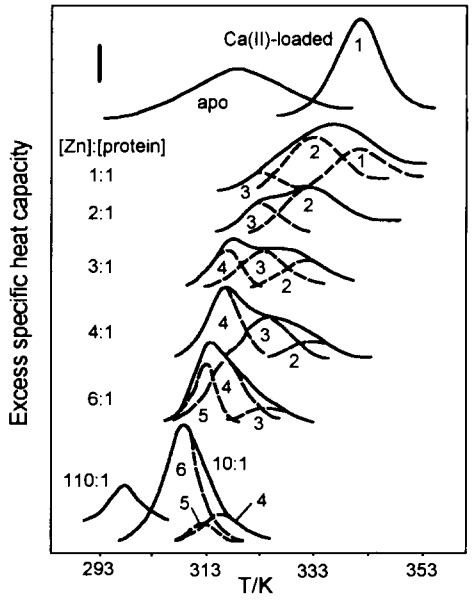

Fig. 7. Heat sorption curves for different states of human α-lactalbumin measured on a DASM-4 microcalorimeter. Protein concentration was 1.3 mg/ml; 10 mM HEPES, pH 7.5. Vertical bar corresponds to 500 J/K kg. The curves measured in the presence of Zn^{2+} were decomposed into elementary components by the successive annealing procedure [56]. The [Zn] : [protein] molar ratios are indicated on each curve. Scan rate was 1 K/min. Curves are displaced along the ordinate for clarity.

Kube et al. [74] studied the thermal denaturation of lactate dehydrogenase from porcine muscle in the apo-form as well as in the form of enzyme–pyruvate, enzyme–NAD^+, and enzyme–NAD–pyruvate–adduct complexes. Pyruvate binding did not affect the thermal stability of lactate dehydrogenase. NAD^+ exerted a stabilizing effect on the enzyme, whose value was proportional to the number of ligand molecules bound per lactate dehydrogenase tetramer. The formation of the abortive lactate dehydrogenase–NAD–pyruvate complex in one, two or three active sites of the enzyme tetramer did not affect the values of the calorimetric parameters of thermal denaturation in comparison with those obtained for the apo-enzyme. The occupancy of all four active sites of lactate dehydrogenase by the adduct resulted in a sharp increase in the thermal stability of the enzyme and tightness of the lactate dehydrogenase–adduct complex as compared with complexes formed during partial saturation. The experimental results point to the existence of a con-

certed conformational transition of the lactate dehydrogenase tetramer induced by the formation of the lactate dehydrogenase–NAD–pyruvate complex in the last active site of the tetramer.

Shnyrov et al. [75] reported the binding of phosphate to *F*-protein (phosphofluctokinase) using the 25°C shift of the denaturating heat capacity peak induced by phosphate.

DSC has been used to study interactions of myosin subfragment 1 with different nucleoside diphosphates and vanadate or beryllium fluoride [76]. In the absence of vanadate or beryllium fluoride, none of the nucleotide diphosphates had much influence on the temperature of the thermal transition although they did increase its sharpness. However, in the presence of vanadate or beryllium fluoride, the effects of Mg^{2+}–NDP complexes were quite different from each other and depended strongly on the base structure of NDP. The authors believe that these calorimetric studies offer a new and promising approach to the investigation of the structural changes occurring in the myosin head due to the formation of M^{**}–NDP–P_i intermediates during Mg^{2+}–NTP hydrolysis.

Fourier transform infrared spectroscopy and DSC have been used to investigate the thermal stability of human serum transferrin, human lactoferrin and rabbit serum transferrin in their diferric and apo forms [77]. The removal of iron leads to thermal destabilization of these proteins. Structural variation in the apo transferrins is indicated by the observation of a single irreversible transition for human apo lactoferrin, a double transition for human serum apo transferrin (one reversible) and a broad irreversible asymmetric transition for rabbit serum apo transferrin.

Regarding the study of biomolecular interactions by DSC, Brandts and Lin [78] have shown that binding and association equilibrium constants can be calculated from the DSC curves corresponding to interacting systems. As shown by these authors, the advantage of this (admittedly indirect) method is that very high equilibrium constants (corresponding to very tight binding or association) may be determined. This is an important result since in most cases no methods are available for determining binding equilibrium constants higher than 10^{13} M^{-1}. Naturally, application of the methodology of Brandts and Lin requires that protein denaturation, as monitored by DSC, be a reversible equilibrium process.

An interesting implication of DSC for protein studies was demonstrated by Sartor et al. [79]. These authors studied the hydration shells of proteins. Their measurements have shown that on reheating at a rate 30 K/min the vitreous but freezable water fraction in methmyoglobin, methemoglobin, and lysozyme powders undergoes, a glass → liquid transition with an onset temperature between 164 and 174 K, a width of 9 to 16 K, and an increase in heat capacity from 20 to 40 J/K. However, the glass transition disappears upon crystallization of the freezable water. These calorimetric features are similar to those of the water embedded in the pores of a synthetic polymer but very different from those of glassy bulk water. The difference with the properties of glassy bulk water is attributed to hydrophilic interaction and hydrogen-bonding of the segments of the macromolecule with the freezable water fraction, which thereby becomes dynamically modified.

Studies of model compounds, such as amino acids, offer insight into the factors affecting the behavior and stability of proteins in aqueous systems. Abate et al. [80] measured the molar heat capacities at constant pressure of the *N*-acetyl-*N'*-methylamides of glycine, *L*- and *DL*-alanine, *DL*-2-aminobutyric acid, *L*- and *DL*-proline, *L*- and *DL*-valine, *DL*-norvaline, *L*- and *DL*-leucine, *DL*-norleucine, *L*- and *DL*-phenylalanine by differential scanning calorimetry from 318 to ca. 20 K below their melting points. The thermal capacity values at 298.15 K of both *L*- and *DL*-amino acid derivatives increase linearly with their molar masses.

4. Applications of microcalorimetry to membrane and protein–membrane systems

The microcalorimetry method is very useful in studies of membrane systems and especially in the study of vesicles formed from synthetic phospholipids, such as dipalmitoylphosphatidylcholine or dimyristoylphosphatidylcholine (see, for review, Ref. [81]). Such vesicles have narrow heat sorption peaks due to phase transition from the gel to the liquid crystalline state. The phase transition temperature and transition enthalpy depend on the chemical structure of lipids.

Wang et al. [82] investigated the interrelationships between phase transition behavior and molecular

structures for monounsaturated phosphatidylcholines. Their combined calorimetric and computational studies led to the conclusion that the melting temperature values of most lipids in two revealed groups can be correlated in an identical manner with their structural parameters and, especially, with the position of a single *cis*-carbon=carbon double bond. Nebylski and Salem [83] studied the gel-to-liquid crystalline phase transitions for a series of mixed-chain unsaturated phosphatidylcholines. They showed that increasing the degree of unsaturation to three or more double bonds resulted in higher transition enthalpy values.

The thermal phase transitions of lipids can be used to regulate the permeability of liposomes. Shevchenko et al. [84] used microcalorimetry to show that exposure of a lipid bilayer to heat causes bilayer melting to form transmembranous single channels at temperatures of the phase transition; this can be used to deliver a drug at the required place at the right time. The conditions for the standardization of liposomes with controlled permeability were defined.

The microcalorimetry method has been used to study the interactions of biologically active compounds with membranes. For example, Gallova et al. [85] have shown that local anesthetics of the homologous series of monohydrochlorides of [2-(alkoxy)phenyl]-2-(1-piperidinyl)ethyl esters of carbamic acid decrease the temperature of the $L'_\beta \rightarrow P_\beta$ (pretransition) and $P_\beta \rightarrow L_\alpha$ (main transition) phase transitions of 1,2-dipalmitoyl-sn-phosphatidylcholine in aqueous phase at pH 6.2. The efficiency of the anesthetics at decreasing the pretransition temperature increases with the number of carbon atoms n of the alkoxy substituent up to $n = 6$. For $n > 6$ no pretransition was detected. The efficiency at decreasing the temperature of the main transition increased up to $n = 8 - 9$ and began to decrease at $n = 10$.

The heat sorption peaks for phospholipid vesicles are sensitive to the state of the membranes used to study interactions between vesicles and different proteins. Permyakov et al. [86,87] studied the interactions of calcium binding proteins, parvalbumin and α-lactalbumin with dipalmitoylphosphatidylcholine vesicles. Interactions of such proteins with vesicles are modulated by calcium and magnesium ions and induce some changes in the physical properties of both the proteins and the vesicles; these are reflected in changes in the heat sorption curves for both vesicles and proteins.

Derksen et al. [88] investigated the thermotropic properties of triolein-rich, low-cholesterol dipalmitoylphosphatidylcholine (DPPC) emulsion particles in the absence and presence of apolipoprotein-A1 by a combination of differential scanning and titration calorimetry. Without the protein on the surface, the heat sorption curve of the emulsion showed three endothermic transitions at 24.3°, 33.0°, and 40.0°C. With apo-A1 on the surface, the heating curve showed the three transitions more clearly. The changes indicate that apo-A1 increases the amount of ordered gel-like phase on the surface of DPPC emulsions when added at 30°C.

Lentz et al. [89] studied the denaturation profiles of bovine prothrombin and its isolated fragments in the presence of membranes containing 1-palmitoyl-2-oleoyl-3-*sn*-phosphatidylcholine in combination with bovine brain phosphatidylserine. Peak deconvolution analysis of the heat sorption curves revealed that membrane binding induces changes in the C-terminal catalytic domain of prothrombin and in a domain that links fragment 1 with the catalytic domain (fragment 2).

Gicquaud [90] has found that actin may interact with membrane lipids. Differential scanning calorimetry shows that when the actin molecule is in contact with distearoylphosphatidylcholine membrane, it undergoes a major conformational change, resulting in the complete disappearance of its phase transition. At the same time, the phase transition of the membrane lipids is only weakly affected by the presence of actin. The interaction is inhibited by high concentrations of KCl, thus indicating that the phenomenon is primarily electrostatic in nature.

Heimburg and Biltonen [91] used the thermotropic behavior of dimyristoylphosphatidyldlycerol membranes to study the interactions of these with cytochrome *c*. In the absence of the protein, the lipid undergoes a sequence of transitions over the 7 to 40°C temperature range. At high lipid concentrations, the heat sorption curves exhibit a pronounced maximum in the excess heat capacity function at about 23°C, with a shoulder on the high-temperature side. The heat capacity curve in the presence of protein is broad with a single maximum. Combination of the microcalorimetry method with viscosimetry, light

scattering, electron microscopy, ESR, and NMR methods permitted the demonstration that at low ionic strength the temperature-dependent polymorphic structure of the lipid is concentration-dependent and is strongly influenced by the presence of protein.

The microcalorimetry method also allows the study of natural membranes. Unlike the situation for water-soluble proteins, fewer experimental studies on the thermodynamics of membrane protein stability have been reported (see, for review, Refs. [92,93]). On the basis of the literature addressing the thermal stability of some membrane proteins, Haltia and Freire [92] concluded that a fundamental difference between soluble and membrane proteins is the high thermal stability of interbilayer secondary structural elements in membrane proteins. This property manifests itself as incomplete unfolding and is reflected in the observed low enthalpies of denaturation of most membrane proteins. Calorimetric studies of membrane protein stability, which can provide definitive values for several thermodynamic parameters affecting protein stability, are complicated by the often irreversible nature of this transition. Despite this, however, very much useful information about membrane organization can be inferred from calorimetric investigations. Thus, Shnyrov [94] carried out calorimetric investigations of $NaBH_4$-modified bacteriorhodopsin in purple membranes from *Halobacterium halobium*. The author showed that two high-temperature peaks beneath the overall endotherms correspond to the process of bacteriorhodopsin denaturation. The results suggest a different structural organization of two populations of bacteriorhodopsin in intact dark-adapted purple membranes.

Shnyrov et al. [95] studied thermal transitions in rat erythrocyte ghosts by scanning microcalorimetry in combination with other methods. Heating of a suspension of rat erythrocyte ghosts induced at least four thermodynamically irreversible transitions induced by thermal stress (Fig. 8). It was shown that the *A* transition is due to an unfolding of spectrin (extraction of spectrin from erythrocyte membranes results in the disappearance of the *A* transition). Treatment of the membranes by papain shifts the *B*-transition toward lower temperatures, which suggests an external location of at least some of the proteins that are unfolded in this transition. The *C* transition was shown to derive from the denaturation of the membrane-spanning

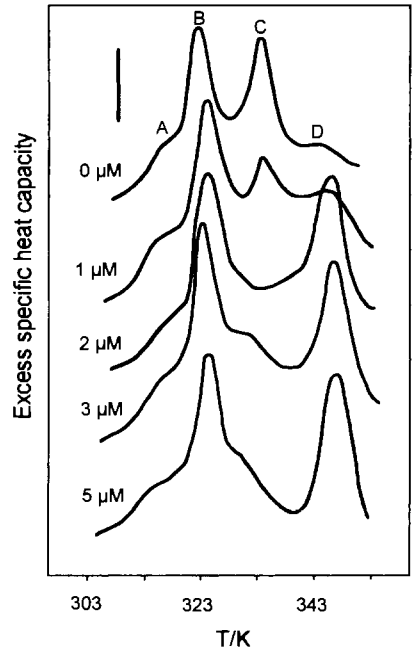

Fig. 8. Calorimetric scans for rat erythrocyte ghosts in the presence of different concentrations of a potent inhibitor of anion transport, DIDS. 5 mM sodium phosphate, pH 7.4. DASM-4 microcalorimeter; scan rate 1 K/min. Curves are displaced along the ordinate for clarity.

domain of the anion transport protein, band 3. The lack of sensitivity of the *C* transition to proteolysis and its high sensitivity to phospholipase suggests that the *C* transition is partially due to lipid melting. Covalent modification of the membranes with the most potent anion transport inhibitor DIDS did not elicit a shift but rather led to the disappearance of the *C* transition (Fig. 8) and to an intensification of the *D* transition. The data presented demonstrate that the microcalorimetry method enables the state of several membrane proteins in erythrocyte ghosts to be monitored.

Shulitova et al. [96] used DSC to study heat inactivation process of O_2 evolution, temperature-induced Mn^{2+} release, and structural transitions in photosystem II-enriched subchloroplast fragments, granal thylakoids and isolated oxygen-evolving pigment-lipoprotein complexes. These authors found that the semi-inactivation temperature of O_2 evolution, which is accompanied with Mn^{2+} release, changes from 45° to 40°C, and 34°C in this series of preparations, in agreement with the decreased structural stability of the

oxygen-evolving pigment-lipoprotein complexes. These studies afford some insight into the molecular basis of the heat sensitivity of the water-oxidizing system of photosystem II chloroplasts.

The microcalorimetry method is quite useful in studies of protein–lipid complexes. Prassl et al. [97] studied human plasma lipoprotein(a) and low-density lipoprotein. Structurally, low-density lipoprotein is a species of quasi-spherical particles consisting of a central core of apolar lipids, mainly esters and triglycerides, stabilized by an external shell of polar lipids, i.e. phospholipids and cholesterol, and a single polypeptide chain, apolipoprotein-B100. Three distinct thermal transitions have been observed for lipoprotein(a): the first one, at ca. 20°C, arises from the core-located apolar lipids; the second one, at 55.7°C, is attributed to apo(a); and the third one, at 80.4°C, corresponds to apo-B100 protein unfolding. The results obtained show that low-density lipoprotein and lipoprotein(a) are similar but not identical in structure and thermal stability, which may be of metabolic interest.

The microcalorimetry method is used to study not only liposomes and biological membranes, but also certain synthetic membranes used in medicine. For example, Ishikiriyama et al. [98] carried out a microcalorimetric study of the freezing and melting behavior of water in 15 types of poly(methyl methacrylate) hydrogel membranes used in artificial kidneys for ordinary hemodialysis, high flux hemodialysis, hemofiltration, and protein-permeable hemofiltration. Pore size distribution curves for the membranes were then calculated from the melting endotherms and the freezing exotherms of the pore water by thermoporosimetry.

5. Use of microcalorimetry in studies of nucleic acids

The microcalorimetry method can be successfully used for studies of the nucleic acids DNA and RNA. For example, Mrevlishvili et al. [99,100] studied the low-temperature heat capacity (2–25 K) of native DNA strands at different humidities. They concluded that the heat capacity of DNA at very low energies (< 1 K) can be correctly described in terms of the generally accepted two-level model. The nature of the excessive density of oscillatory states at energies 3 to 10 K is related to oscillatory excitations in structural inhomogeneities, which can be clusters of hydrated water molecules on the DNA matrix.

Plum and Breslauer [101] thermodynamically characterized the melting transitions of a DNA 31-mer oligonucleotide, which was designed to fold into an intramolecular triple helix. They found that the 31-mer exhibits either one or two melting transitions, depending on the conditions of the solution. DSC was used to determine the energetics of the two transitions between the three structural states; namely, the triplex-to-hairpin duplex transition, and the hairpin duplex-to-coil transition. By combining spectroscopic and calorimetric data, they developed a semi-empirical model which describes the state of the 31-mer as a function of pH, sodium ion concentration, and temperature.

6. Use of microcalorimetry in studies of polysaccharides

Polysaccharides can be studied by differential scanning calorimetry. Ratto et al. [102] measured the transition temperatures of water/chitosan (deacetylated chitin, which is a naturally occurring linear polymer of $\beta(1 \rightarrow 4)$poly-*N*-acetylglucosamine) systems with water contents ranging from 8 to 300% by DSC. Three kinds of phases that varied with the water content were observed for the system: cold crystallization, the melting of freezable water, and the birefringent-to-isotropic phase, which occurs for samples containing 44 to 190% water, with a transition temperature that does not vary significantly with the water content.

7. Use of microcalorimetry in studies of cells and tissues

The microcalorimetry method can be successfully used to study on cells and even tissues. Figs. 3 and 9 show the thermograms of cock sperm. The heat sorption curve in Fig. 3 was decomposed into elementary components corresponding to the melting of protein domains and DNA by the successive annealing procedure. Fig. 9 demonstrates results of a microca-

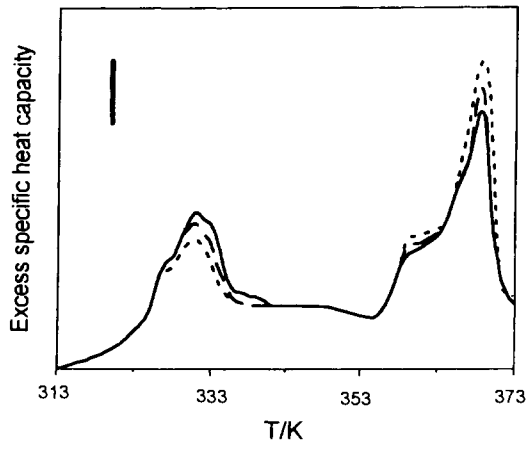

Fig. 9. Heat sorption curves for a suspension of cock sperm: (———) – intact cells; (- - -) – cell suspension treated by cryoprotectors; and (· · ·) – cell suspension after freezing and thawing; DASM-4 microcalorimeter; scan rate 1 K/min.

lorimetric study of effects of cryoprotectors and freezing and thawing on the nativity of spermatozoa [103].

Gutsze et al. [104] used ^{1}H NMR and scanning calorimetry methods to study water in rabbit eye lenses. Using calorimetry, it was shown that the lenses can be easily undercooled to temperatures well below the freezing point of water. The maximum achievable undercooling temperature of the lens is a function of the cooling rate. The authors believe that any previous discussions about the specific value of the temperature of water crystallization in biological systems should be carefully reconsidered.

Oreshkin et al. [105–107] studied the heat-induced structural changes in the proteins of bovine muscle and the effects of technological meat treatment on the thermal denaturation of meat proteins. The microcalorimetry method enabled them to monitor the processes of thermal denaturation and coagulation of the meat proteins. The data obtained were used to optimize the technology of the heat treatment of meat. For other applications of DSC in the control of the processing and storage of amorphous foods, the reader is referred to [108].

Bogomolov and Bikbov [109] used DSC to study soybean germination. The existence of a special conformational state for the 11 S storage protein was detected in the storing state of the seed. During seed germination the storage protein undergoes certain conformational rearrangements that can be detected by reading with DSC.

Physiological changes in 'Hakuho' peach flower buds during endodormancy and ectodormancy were investigated based on their water status as measured by DSC and NMR spectroscopy [110]. The developmental stage in ectodormancy, which was estimated as the number of days between the sampling date for shoots and the bloom date after forcing, was dominated by the absorption of water.

References

[1] P.L. Privalov, Adv. Protein Chem., 33 (1979) 167.
[2] P.L. Privalov, Adv. Protein Chem., 35 (1982) 1.
[3] P.L. Privalov, Annu. Rev. Biophys. Chem., 18 (1989) 47.
[4] J.M. Sturtevant, Ann. Rev. Phys. Chem., 38 (1987) 463.
[5] E. Freire, W.W. van Osdol, O.L. Mayorga and J.M. Sanchez-Ruiz, Ann. Rev. Biophys. Biophys. Chem., 19 (1990) 159.
[6] E. Freire, Methods Enzymol., 259 (1995) 144.
[7] J.M. Sanchez-Ruiz, in: S. Roy and B.B. Biswas (Eds.), Subcellular Biochemistry, Vol. 24, Plenum Press, New York, 1995, p. 133.
[8] G.I. Makhatadze and P.L. Privalov, Adv. Prot. Chem., 47 (1995) 307.
[9] J. Gomez, V.J. Hilser, D. Xie and E. Freire, Proteins: Structure, Function and Genetics, 22 (1995) 404.
[10] P.L. Privalov and G.I. Makhatadze, J. Mol. Biol., 224 (1992) 715.
[11] P.L. Wintrode, G.I. Makhatadze and P.L. Privalov, Proteins: Structure, Function and Genetics, 18 (1994) 246.
[12] G.I. Makhatadze, G.M. Clore, A.M. Gronenborn and P.L. Privalov, Biochem., 33 (1994) 9327.
[13] A.M. Klibanov and T.J. Ahern, in: D.L. Oxender and C.F. Fox (Eds.), Protein Engineering, Alan R. Liss, New York, 1987, p. 213.
[14] D. Baker and D.A. Agard, Biochem., 33 (1994) 7505.
[15] S.P. Manly, K.S. Matthews and J.M. Sturtevant, Biochem., 24 (1985) 3842.
[16] J.M. Sanchez-Ruiz, Biophys. J., 61 (1992) 921.
[17] J.R. Lepock, A.M. Rodahl, M.L. Zhang, M.L. Heynen, B. Waters and K.H. Cheng, Biochem., 29 (1990) 681.
[18] J.M. Sanchez-Ruiz, J.L. Lopez-Lacomba, M. Cortijo and P.L. Mateo, Biochem., 27 (1988) 1648.
[19] J.M. Sanchez-Ruiz, J.L. Lopez-Lacomba, P.L. Mateo, M. Vilanova, M.A. Serra and F.X. Aviles, Eur. J. Biochem., 176 (1988) 225.
[20] M. Guzman-Casado, A. Parody-Morreale, P.L. Mateo and J.M. Sanchez-Ruiz, Eur. J. Biochem., 188 (1990) 181.
[21] P.E. Morin, D. Diggs and E. Freire, Biochem., 29 (1990) 781.
[22] M.L. Galisteo, P.L. Mateo and J.M. Sanchez-Ruiz, Biochem., 30 (1991) 2061.

[23] F. Conejero-Lara, P.L. Mateo, F.X. Aviles and J.M. Sanchez-Ruiz, Biochem., 30 (1991) 2067.
[24] F. Conejero-Lara, J.M. Sanchez-Ruiz, P.L. Mateo, F.J. Burgos and F.X. Aviles, Eur. J. Biochem., 220 (1991) 663.
[25] M.L. Galisteo and J.M. Sanchez-Ruiz, Eur. Biophys. J., 22 (1993) 25.
[26] T. Le Bihan and C. Gicquaud, Biochem. Biophys. Res. Commun., 194 (1993) 1065.
[27] G.G. Zhadan and V.L. Shnyrov, Biochem. J., 299 (1994) 731.
[28] D.I. Kreimer, V.L. Shnyrov, E. Villar, I. Silman and L. Weiner, Prot. Sci., 4 (1995) 2349.
[29] A.L. Garda-Salas, R.I. Santamaría, M.J. Marcos, G.G. Zhadan, E. Villar and V.L. Shnyrov, Biochem. Mol. Biol. Internat., 38 (1996) 161.
[30] V.L. Shnyrov, M.J. Marcos and E. Villar, Biochem. Mol. Biol. Internat., 39 (1996) 647.
[31] C.A. Miles, T.V. Burjanadze and A.J. Bailey, J. Mol. Biol., 245 (1995) 437.
[32] L. Serrano, J.T. Kellis, P. Cann, A. Matouschek and A.R. Fersht, J. Mol. Biol., 224 (1992) 783.
[33] M.M. Santoro and D.W. Bolen, Biochem., 31 (1992) 5278.
[34] C.M. Johnson and A.R. Fersht, Biochem., 34 (1995) 6795.
[35] B. Ibarra-Molero and J.M. Sanchez-Ruiz, Biochem., 35 (1996) 14689.
[36] J.K. Myers, N. Pace and J.M. Scholtz, Prot. Sci., 4 (1995) 2138.
[37] Y. Liu and D.W. Bolen, Biochem., 34 (1995) 12884.
[38] G.I. Gitelson, Y.V. Griko, A.V. Kurochkin, V.V. Rogov, V.P. Kutyshenko, M.P. Kirpichnikov and P.L. Privalov, FEBS Lett. , 289 (1991) 201.
[39] Y.V. Griko, V.V. Rogov and P.L. Privalov, Biochem., 31 (1992) 12701.
[40] J.C. Martinez, V.V. Filimonov, P.L. Mateo, G. Schreiber and A.R. Fersht, Biochem., 34 (1995) 5224.
[41] G.I. Makhatadze, K.S. Kim, C. Woodward and P.L. Privalov, Prot. Sci., 2 (1993) 2028.
[42] P.L. Privalov and G.I. Makhatadze, J. Mol. Biol., 232 (1993) 660.
[43] W.A. Lim, D.C. Farmggio and R.T. Sauer, Biochem., 31 (1992) 4324.
[44] C.N. Pace, J. Mol. Biol., 226 (1992) 29.
[45] C. Steif, H.J. Hinz and G. Cesareni, Proteins: Structure, Function and Genetics, 23 (1995) 83.
[46] J.E. Ladbury, R. Wynn, J.A. Thomson and J.M. Sturtevant, Biochem., 34 (1995) 2148.
[47] J.R. Liggins, F. Sherman, A.J. Mathews and B.T. Nall, Biochemistry, 33 (1994) 9209.
[48] C.Q. Hu, S. Kitamura, A. Tanaka and J.M. Sturtevant, Biochem., 31 (1992) 1643.
[49] M.M. Santoro, Y. Liu, S.M.A. Khan, L.-X. Hou and D.W. Bolen, Biochem., 31 (1992) 5278.
[50] A. Wang, A.D. Robertson and D.W. Bolen, Biochem., 34 (1995) 15096.
[51] S.N. Timasheff, in: C.V. Osmond, C.L. Bolis and G.N. Somero (Eds.), Water and Life: Comparative Analysis of Water Relationships at the Organic, Cellular, and Molecular Levels, Springer-Verlag, Berlin, 1992, p. 70.
[52] I.M. Plaza del Pino and J.M. Sanchez-Ruiz, Biochem., 34 (1995) 8621.
[53] K.P. Murphy and S.J. Gill, J. Mol. Biol., 222 (1991) 699.
[54] V.L. Shnyrov, D.I. Levitsky, N.S. Vedenkina, O.P. Nikolaeva, N.V. Khvorov, E.A. Permyakov and B.F. Poglazov, Dokl. Acad. Nauk SSSR (Russian), 304 (1989) 1497.
[55] D.I. Levitsky, N.V. Khvorov, V.L. Shnyrov, N.S. Vedenkina, E.A. Permyakov and V.F. Poglazov, FEBS Lett., 264 (1990) 176.
[56] V.L. Shnyrov, G.G. Zhadan and I.G. Akoev, Bioelectromagnetics, 5 (1984) 411.
[57] D.I. Levitsky, V.L. Shnyrov, N.V. Khvorov, A.E. Bukatina, N.S. Vedenkina, E.A. Permyakov, O.P. Nikolaeva and B.F. Poglazov, Eur. J. Biochem., 209 (1992) 829.
[58] M. Nakaya and S. Watabe, Biochem., 34 (1995) 3114.
[59] E.A. Permyakov, V.L. Shnyrov, L.P. Kalinichenko and N.Y. Orlov, Biophys. Acta, 830 (1985) 288.
[60] A. Tanaka, H. Fukada and K. Takahami, J. Biochem., 117 (1995) 1024.
[61] S.P. Martsev, Z.I. Kravchuk and A.P. Vlasov, Immunology Lett., 43 (1994) 149.
[62] P.M. Coll, P. Perez, E. Villar and V.L. Shnyrov, Biochem. Mol. Biol. Internat., 34 (1994) 1091.
[63] A. Ruiz-Arribas, R.I. Santamaría, G.G. Zhadan, E. Villar and V.L. Shnyrov, Biochem., 33 (1994) 13787.
[64] G. Damaschun, H. Damaschun, K. Gast, R. Misselwitz, J.J. Muller, W. Pfeil and D. Zirwer, Biochem., 32 (1993) 7739.
[65] A.R. Viguera, J.C. Martinez, V.V. Filimonov, P.L. Mateo and L. Serrano, Biochem., 33 (1994) 2142.
[66] A. Musatov, E.A. Permyakov, J. Bagelova, L.A. Morozova and V.L. Shnyrov, Biochem. Internat., 21 (1990) 563.
[67] L.A. Morozova, V.L. Shnyrov, N.V. Gusev and E.A. Permyakov, Biokhimia (Russian), 53 (1988) 531.
[68] L.A. Morozova, V.L. Shnyrov, N.V. Gusev and E.A. Permyakov, in: L.M.G. Heilmeyer, Jr. (Ed.), NATO ASI Series, H 56, Cellular Regulation by Protein Phosphorylation, Springer Verlag, 1991, p. 67.
[69] V. Karantza, A.D. Baxevanis, E. Freire and E.N. Moudrianakis, Biochem., 34 (1995) 5988.
[70] C.R. Johnson, P.E. Morin, C.H. Arrowsmith and E. Freire, Biochem., 34 (1995) 5309.
[71] K.G. Davis, S.E. Plyte, S.R. Robertson, A. Cooper and G.G. Kneale, Biochem. , 34 (1995) 148.
[72] E.A. Permyakov, V.L. Shnyrov, L.P. Kalinichenko, A. Kuchar, I.L. Reizer and L.J. Berliner, J. Prot. Chem., 10 (1991) 577.
[73] N.S. Vedenkina, A.A. Abramyan, Z.N. Bagdasaryan, V.L. Shnyrov and E.A. Permyakov, Biokhimia (Russian), 56 (1991) 500.
[74] D. Kube, V.L. Shnyrov, E.A. Permyakov, M.V. Ivanov and N.K. Nagradova, Biokhimia (Moscow), 52 (1997) 1116.
[75] V.L. Shnyrov, N.A. Freidina and E.A. Permyakov, Biochim. Biophys. Acta, 953 (1988) 128.
[76] A.A. Bobkov and D.I. Levitsky, Biochem., 34 (1995) 9708.

[77] J.M. Hadden, M. Bloemendal, P.I. Haris, S.K.S. Srai and D. Chapman, Biochim. Biophys. Acta, 1205 (1994) 59.
[78] J.F. Brandts and L.N. Lin, Biochem., 29 (1990) 6927.
[79] G. Sartor, A. Hallbrucker and E. Mayer, Biophys. J., 69 (1995) 2679.
[80] L. Abate, G. Della Gatta and G. Somsen, Thermochim. Acta, 239 (1994) 7.
[81] R.N. McElhaney, Biochem. Biophys. Acta, 864 (1986) 361.
[82] Z. Wang, H. Lin, S. Li and C. Huang, J. Biol. Chem., 270 (1995) 2014.
[83] C.D. Nebylski and N. Salem Jr., Biophys. J., 67 (1994) 2387.
[84] E.V. Shevchenko, E.Y. Smirnova, M.L. Kakushkina, D.A. Predvoditelev and V.F. Antonov, Pharmacy, 42 (1993) 7.
[85] J. Gallova, J. Bagelova, J. Cizmarik and P. Balgavy, Coll. Czech. Chem. Commun., 60 (1995) 763.
[86] E.A. Permyakov, D.I. Kreimer, L.P. Kalinichenko and V.L. Shnyrov, Gen. Physiol. Biophys., 7 (1988) 95.
[87] E.A. Permyakov, D.I. Kreimer, L.P. Kalinichenko, A.A. Orlova and V.L. Shnyrov, Cell Calcium, 10 (1989) 71.
[88] A. Derksen, D. Gantz and D.M. Small, Biophys. J., 70 (1996) 330.
[89] B.R. Lentz, C.M. Zhou and J.R. Wu, Biochem., 33 (1994) 5460.
[90] C. Gicquaud, Biochem., 32 (1993) 11873.
[91] T. Heimburg and R.L. Biltonen, Biochem., 33 (1994) 9477.
[92] T. Halia and E. Freire, Biochim. Biophys. Acta, 1241 (1995) 295.
[93] M.H.B. Stowell and D.C. Rees, Adv. Prot. Chem., 46 (1995) 279.
[94] V.L. Shnyrov, Biochem. Mol. Biol. Internat., 34 (1994) 281.
[95] V.L. Shnyrov, C.H. Salija, G.G. Zhadan and E.A. Permyakov, Biochim. Biomed. Acta, 45 (1986) 1111.
[96] N. Shulitova, G. Semenova, V. Klimov and V. Shnyrov, Biochem. Mol. Biol. Internat., 35 (1995) 1233.
[97] R. Prassl, B. Schuster, P.M. Abuja, M. Zechner, G.M. Kostner and P. Laggner, Biochem., 34 (1995) 3795.
[98] K. Ishikiriyama, M. Todoki, T. Kobayashi and H. Tanzawa, J. Coll. Interface Sci., 173 (1995) 419.
[99] G.M. Mrevlishvili, Biofizika (Russian), 40 (1995) 485.
[100] G.M. Mrevlishvili, L.L. Buishvili, G.S. Dzhaparidze and G.P. Kakabadze, Biofizika (Russian), 40 (1995) 518.
[101] G.E. Plum and K.J. Breslauer, J. Mol. Biol., 248 (1995) 679.
[102] J. Ratto, T. Hatakeyama and R.B. Blumstein, Polymer, 36 (1995) 2915.
[103] A.V. Tereschenko and V.L. Shnyrov, Sci. Bull. (Russian), 24 (1988) 33.
[104] A. Gutsze, J. Bodurka, R. Olechnowicz, G. Buntkowsky and H.H. Limbach, Z. Naturforsch., 50c (1995) 410.
[105] E.F. Oreshkin, M.A. Borisova, G.S. Tchubarova, V.M. Gorbatov, E.A. Permyakov, V.L. Shnyrov and E.A. Burstein, Meat Science, 16 (1986) 297.
[106] E.F. Oreschkin, M.A. Borissowa, E.A. Permjakow, E.A. Burstein and V.L. Schnyrow, Fleischwirtschaft, 65 (1985) 1498.
[107] E.F. Oreschkin, M.A. Borissowa, E.A. Permjakow and E.A. Burstein, Fleischwirtschaft, 69 (1989) 627.
[108] M. Karel, A. Anglea, P. Buera, R. Karmas, G. Levi and Y. Roos, Thermochim. Acta, 246 (1994) 249.
[109] A.A. Bogomolov and T.M. Bikbov, Biokhimia (Russian), 60 (1995) 626.
[110] T. Sugiura, M. Yoshida, J. Magoshi and S. Ono, J. Amer. Hort. Sci., 120 (1995) 134.